Proceedings of the Institute of Acoustics

ACOUSTIC TOMOGRAPHY OF ROUGH SEA SURFACE

I B Burlakova, Yu A Dubovoy, A L Zeigman, A G Nechayev, M M Slavinsky, and N M Smirnov

Institute of Applied Physics, USSR Academy of Science, Nizhny Novgorod, USSR

ABSTRACT

A method for acoustic diagnostics of wind waves in large acquatoria using the transmission scheme of tomography is considered. Swell parameter estimates are given based on the angular-frequency spectrum measurements of the signal on one acoustic path. Results of the experiment are reported.

There have recently been many experiments on acoustic tomograppy of the ocean to investigate the processes in the ocean medium and to develop a variety of tomography of the rough sea surface [2,3].This paper shows a possible way to solve the inverse problem using the transmission scheme of tomography [4].
Results of the experiment, in which the space-averaged swell and wind wave parameters are determined by acoustic measurements on a long path, are reported.

Consider a surface sound channel 1 (Fig 1a) with sound velocity profile C(z) (z is the vertical coordinate) independent of the horizontal variables (x,y).We assume that the heights of the sea surface irregularities are small enough to meet the Rayleigh parameter smallness condition $P \ll 1$ [1] and allow mode representation of the sound field to be used [1,6]. The sea roughness is assumed to be quasihomogeneous $G \gg 1$, where l is the spatial correlation radius and G is a characteristic variation scale of the roughness parameters. Characteristic of a sound source and receiver are the mode intensity excitation coefficients $a_s(n)$ and $a_r(n)$ (n - mode number).

First we discuss the possibility of using the tomographic scheme to define the sea roughness parameters (wave height, period and propagation direction and roughness angular and frequency spectrum width). The sound scattering effects at rough sea surface leads to an additional decrease in energy of the coherent component (time-averaged) of the acoustic field, the appearance of a fluctuation component in the signal, and the broadening of its angular and frequency spectra [1,5-7]. The roughness parameter variation along the acoustic path changes the evoluti-

ACOUSTIC TOMOGRAPHY OF ROUGH SEA SURFACE

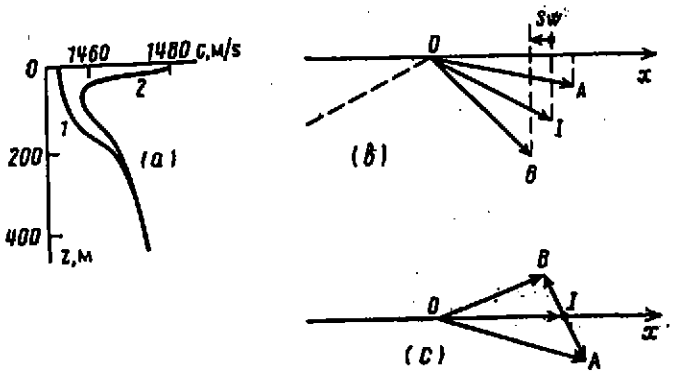

Fig.1 a) Winter (1) and summer (2) profiles of sound velocity; b) scattering of a plane sound waves by roughness (vertical view):OI is the projection of the wave vector of the wave reflected in the mirror direction, $\angle XOI = \theta_i$, OA and OB are the projections of the waves vectors of the scattered components $k_s^{(1)}$ and $k_s^{(2)}$, $\angle XOA = \theta_s^{(1)}$, $\angle XOB = \theta_s^{(2)}$; sw is the projectoin of the wave vector of roughness k_{sw}; c) is the scattering of a plane sound wave by swell (horizontal view): OI is the projection of the wave vector of the incident wave, OA and OB are the projections of the wave vectors of the scattered components $k_s^{(1)}$ and $k_s^{(2)}$ $\angle BOI = +\delta$, $\angle AOI = -\delta$, IB is the wave vector of k_{sw}

on of the energy spectrum characteristics of the signal. Let the statatistic characteristic $\bar{B}_\nu$ (signal projection), measuered by the receiver, be

$$\bar{B}_\nu = Q_\nu \int_{\mathfrak{L}_\nu} B(x,y,z)\,d\lambda \quad . \qquad (1)$$

where Q_ν^{-1} is the total length of the path, ν is the number of the trajectory $\mathfrak{L}_\nu$ or the projection (which defines the source and receiver pair). Based on the results of the papers [1,5-7] it can be shown that with appropriate choice of the signal emission and reception conditions (distributions $a_s(n)$ and $a_r(n)$) this property corresponds to the attenuation coefficient

ACOUSTIC TOMOGRAPHY OF ROUGH SEA SURFACE

γ of the coherent field component and $\Delta f_j / \Delta l_j$, where Δf_j is the frequency spectrum width of the signal of a monochromatic source on passing a segment of length Δl_j ($l << \Delta l_j << G$). For example, γ satisfies (1) when $a_s(n)$ or $a_r(n)$ are sharp functions of n, and $\Delta f_j^2 / \Delta l_j$ - when $a_s(n)$ is proportional to the mode energy distribution on asymptotically long paths [6,7].

In the general case of sound scattering due to anisotropic roughness the field parameter $B(x,y,\nu)$ is a function of not only the coordinates (x,y), but also of the sound propagation direction. Suppose, however, that $B(x,y,\nu)=B(x,y)$ is independent of the orientation of the path through the point (x,y). In particular, this condition is met for isotropic roughness. Then the integral equation (1) (Radon's transform) with respect to $B(x,y)$ can be solved using the well-known algorithms [4,8]. To restore the two-dimensional structure of $B(x,y)$ by a discrete set of projections $\bar{B}_\nu$ is essentially to calculate the space-averaged values B_m in each elementary cell (m is the number of the cell) into which the region is divided. The minimum size of the cell depends on the path number and position, and on the sound scattering efficiency at rough surface in real situations. In the experiment described below the spatial resolution was about 100 km. The rough surface parameters in each cell are defined from the calculated values B_m in accordance with the dependences of the statistic signal characteristics [1,5-7]. It is radically important to use the information on the structure of the angular-frequency spectrum of sea roughness known a priori.

For developed isotropic wind waves all the characteristics are unambiguously related to the wind velocity V near surface [9]. In this case from the solution (1) with respect to attenuation caefficient γ_V or width of the freguency spectrum Δf_V it is possible to determine, in terms of the isotropic roughness model for a given cell, the effective wind velocity V from which other characteristics of roughness can be found.

Since the spatial variation of the swell parameters is small, the swell diagnostics does not require the use of the tomographic principle, so that one acoustic path is sufficient. On long paths the sound attenuation due to scattering by swell can in many cases be described in the first approximation of the small perturbation method [1,6]. Attenuation coefficient γ_{sw} of the coherent component of the sound depending on swell parameters

ACOUSTIC TOMOGRAPHY OF ROUGH SEA SURFACE

(where k_{sw} is the wave number of the swell, $f_{sw} = (gk_{sw})^{0.5} 2\pi$ is the frequency, H is the r.m.s. height, ψ_{sw} is the angle between the swell and the sound propagation directions , and $\Delta\psi << 1$ is the angular spectrum width) was obtained in [2,11] using this approximation. Differentiation between groups of lower and higher modes (formation of sharp distributions $a_{sw}(n)$ or $a_{sw}(n)$) or the use of multifrequency radiation allow the unknowns H, ψ_{sw} (or $\pi \pm \psi_{sw}$) and $\Delta\psi$ to be defined unambiguously from a few values of γ_{sw} [2]. Note that in the case of interest, at $|\psi_{sw}| \simeq 90^{\circ}$, we have: $\gamma_{sw} \cong P_p / x P_k$, where P_p and P_k are intensities of the scattering and coherent components of the sound, x is the path length [2].

The angular-frequency spectrum of swell is fairly narrow. The components of different scattering multiplicity in the signal spectra practically do not overlap so that on long paths it is possible to separate a singly scattered component of the sound. The resonance scattering condition implies [1,10] (see also Fig.1 and the caption) that different parts of the frequency and angular (in a horizontal plane) spectra of the signal at $|\pi/2 - |\psi_{sw}|| > \Delta\psi$ are formed by different groups of modes (the rays at angles $\theta_s^{(1)}$ correspond to modes with lower numbers and the rays at $\theta_s^{(2)}$, to modes with higher numbers than those corresponding to a ray with a grazing angle θ_i). Depending on the quadrant, in which the vector k_{sw} lies, one of four mutually unambiguous correspondences between the frequency ($f_i \pm f_{sw}$) and angular components of the scattered field in a horizontal ($\pm\delta$) and a vertical ($\theta_s^{(1)}$ and $\theta_s^{(2)}$) plane always occurs. For the case shown in Figs. 1b and 1c the component scattered at an angle $\theta_s^{(1)}$ has a frequency $f_i - f_{sw}$ and enters the receiver at an angle $-\delta$ while the component $k_s^{(2)}$ has a frequency $f_i + f_{sw}$ and comes at an angle $+\delta$. If $|\pi/2 - |\psi_{sw}|| < \Delta\psi$, then the angles $\theta_s^{(1)}$ and $\theta_s^{(2)}$ are close to θ_i. In each group of modes (lower and higher) the scattered field contains both frequency ($f_i \pm f_{sw}$) and both angular ($\pm\delta$) components between which there is also one of two (depending on the sign of ψ_{sw}) mutually unambiguous correspondences. Thus,

ACOUSTIC TOMOGRAPHY OF ROUGH SEA SURFACE

by analyzing the angular and frequency spectra of the signal we can define the quadrant in which the vector k_{sw} lies.

The scheme of acoustic tomography of a rough sea surface was tested experimentally in the surface sound channel 1 (Fig 1a) in 1984 [2].

The mean sea depth was 5 km. The ship with a towed system of three high-stability transducers, the frequencies of which covered a bioctave range, receded from the receiving hydrophones in the shelf. The hydrological and meteorological analysis was performed by measurements from the emitting ship (Fig. 2) and using the synoptic data. In time intervals II and IV (Fig.2) the wind velocity V from the source to the receiver decreased by a few m/s and remained almost unchanged in regions I and III. An oceanic swell with parameters H = 0.5 - 0.7 m and $\psi_{sw} \cong 90^{o}$ and a period T $\cong$ 9 s was observed on the whole path. The signal processing aimed at obtaining the power spectra of 500 s realizations by which the statistic characteristics of the signal were found. Figure 3 shows typical noncoherently averaged spectra S(f) of the signals (M is the number of averagings). In the averaging the spectra were tuned to one carrier frequency to decrease the influence of slow velocity variations of the emitting system. The velocity fluctuations define the path length-independent spectrum width Δf_o of the emitted signal, and therefore of the coherent field [12].

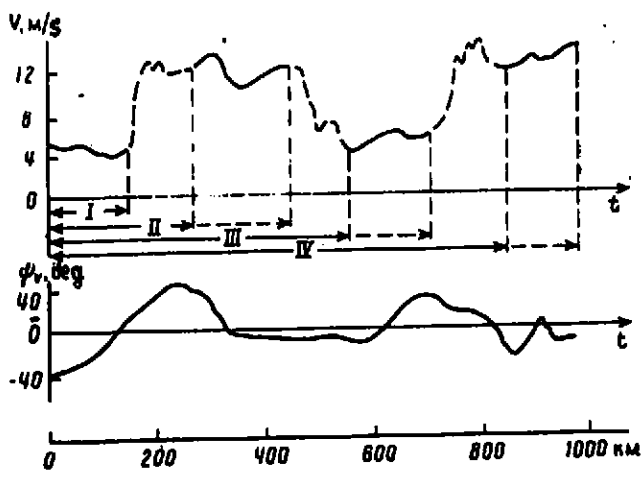

Fig.2 Time dependences of wind velocity V and wind direction ψ_V at the site of the emitting vessel. The lower horizontal axis is the distance between the source and the receiver.

ACOUSTIC TOMOGRAPHY OF ROUGH SEA SURFACE

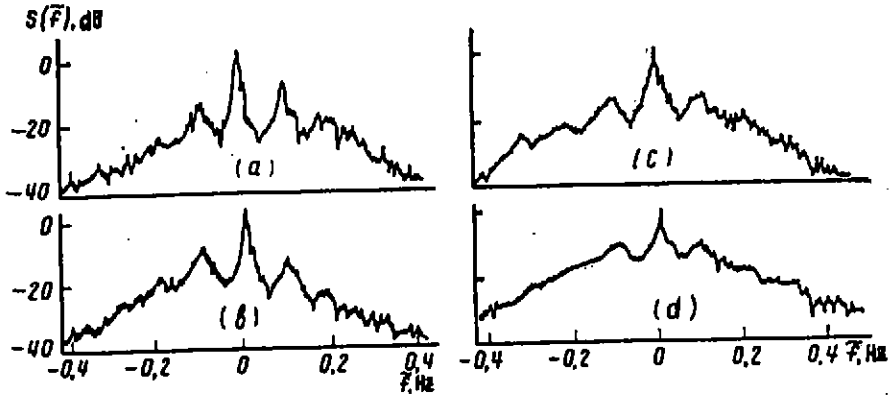

Fig.3 Averaged frequency spectra S(f) of the signal at weak a), b) (alternate phasing of signals in the group of horizontal hydrophones) and at strong wind c), d) (reception with a single hydrophone): a) - path III, x = 566-579 km, M = 52, $\delta > 0$; b) - path III, x = 566-579 km, M = 52, $\delta < 0$; c) - path II, x = 340-408 km, M = 54; d) - path IV, x = 830-887 km, M = 50.

Besides the central coherent component in the range $|\tilde{f}| = |f-f_i| \leq 0.05$ Hz, lateral fluctuation components are seen in the spectra.The relative contribution of the fluctuation field grows with increasing path length at the same wind velocity. At weak wind the scattered field spectrum consists of rather narrow side harmonics with the frequencies of the energy-carrying components $\tilde{f} \cong \pm 0.1$ Hz (it should be natural to explain these harmonics by the single scattering of sound on swell). A change in phasing of jointly processed signals in the group of horizontal hydrophones leads to a change in relative contribution of the side components (Figs. 3a and 3b). At strong wind the relative level of a wide frequency "pedestal" $0.05 \text{ Hz} \leq |\tilde{f}| \leq 0.4$ Hz) increases noticeably because of the sound scattering due to wind roughness. Thus, it is seen that the scattered component contribution depends on path length, wind force and signal phasing.

To define the roughness parameters and compare them with the meteorological data we chose acoustic paths I, II, III and IV (Fig. 2) at about the same wind, with relative stability of the signal characteristics.Path segments where wind changed and tho-

se corresponding to the roughness onset time were disregarded. In the chosen time intervals, it should be reasonable to assume that the sea roughness is stationary (but inhonmogeneous along the path). Thus, we can use the well-known relationship [9] between developed wind waves and wind velocity.

By arrangement of the side component maxima on paths I and III we defined a characteristic period of swell $T = f_{sw}^{-1} \cong 10$ s. Calculation of the distributions $a_s(n)$ and $a_r(n)$ showed that most energy of the sound field, when excited, was concentrated in the lower modes, and a similar group of modes (corresponding to rays with grazing angles on water surface $\theta < 0.09$) was used when the signal was received (in the shelf). This fact (i.e $\theta_s \cong \theta_i$) and the same amplitudes of the scattered components at $\tilde{f} \cong \pm f_{\sigma\omega}$ with nonhorizontal reception imply that $|\psi_{sw}| \cong 90^\circ$. From the calculation based on [1,5] it follows that at weak wind ($V \cong 5$ m/s) the attenuation coefficient of the intensities P_k and P_p on wind waves are almost the same, i.e. the ratio P_p/P_k is independent of the wind wave parameters. Therefore, we estimated γ_{sw} by the experimantal values of the intensities P_k and P_p, which were defined from the frequency spectrum of the field at $|\tilde{f}| \leq 0.05$ Hz for P_k and at $0.05 \leq |\tilde{f}| \leq 0.15$ Hz for P_p. At one frequency we found $\gamma_{sw} \simeq (1.2 \pm 0.4)\ 10^{-3}$ km^{-1} on path I and γ_{sw} $(1 \pm 0.25)\ 10^{-3}$km^{-1} on path III. Using Eqs. for coefficient γ_{sw} obtained in [2,11] we found $H \cong 0.7 - 0.75$ m on paths I and III at different frequencies because of the insufficient accuracy in measurement (in estimating H we took $\Delta\psi \simeq 10^\circ$). The positive sign of ψ_{sw} was revealed by domination of scattered components at $\tilde{f} = + f_{sw}$ over those at $\tilde{f} = - f_{sw}$ (Figs. 3a and 3b) with corresponding ($\delta > 0$) phasing of jointly processed signals in the group of horizontal hydrophones.

Analysis of the deviation of ψ_V on the whole path (from Fig.2 it is seen that the deviation of ψ_V reached 40° only at the emission points) showed that a wind wave model with a homogeneous (-90° - $+90^\circ$) angular energy distribution can be used for the whole path on the average. Therefore, an isotropic roughness model is appli-

cable. Comparison of the powers of the coherent field components obtained at the same wind velocity but on different path lengths makes it possible to find the experimental value of the attenuation coefficient γ of the coherent field intensity.This attenuation coefficient consists of three terms: $\gamma = \gamma_{Vad}+\gamma_{sw}+\gamma_V$, when γ_{Vad}takes into account the attenuation not related to the sound scattering at rough surface. Measurements in this part of the ocean in a summer-type channel 2 (Fig. 1a), where the sea roughness influence was insignificant, indicated that the sound attenuation (the coefficient γ_{Vad}) is best described by Vadov's empirical formula [13]. From the experimental values of γ,γ_{sw}(on paths II and IV the value of γ_{sw} was taken the same as that at weak wind) and γ_{Vad} we calculated the coefficients γ_V , and from the linear losses of the coherent field $\beta = 4.3\gamma_V$ (see Fig. 4a) we defined the path-averaged wind velocities V $\simeq$10-11 m/s (paths II and IV) and V $\simeq$ 5 - 6 m/s (paths I and III).

Calculation using the equations taken from [7] for the experimental conditions shows that width of the freguency spectrum is

$$\Delta f = \sqrt{\Delta f_o^2 + \Delta f_{sw}^2 + \Delta f_V^2}$$

where $\Delta f_{o,sw,V}$ are the widths of the freguency spectrum of the emitted signal, the harmonic source signal scattered by swell only and the harmonic source signal scattered by wind waves only, respectively.

The quantity Δf_o was taken in accordance with the experimental measurements in channel 2 (Fig. 1a). The estimate of Δf_{sw} was obtained under the assumption that the swell-scattered field component in the frequency spectrum is represented as a sum of two δ-functions of power $0.5P_p \simeq 0.5P_k\gamma_{sw}x$, each at frequences $\tilde{f}= \pm f_{sw}$; $\Delta f_{sw}=f_{sw}(\gamma_{sw}x)^{0.5}$.At weak wind (paths I and III), when the wind wave influence on the frequency spectrum width is insignificant, $\Delta f_V \simeq 0$ (almost the whole energy scattered by wind waves is emitted from the channel), the measured value of Δf agrees well with the value calculated from Δf_o and Δf_{sw}.Using the experimental values of Δf and Δf_o and the estimate of Δf_{sw} for paths II and

ACOUSTIC TOMOGRAPHY OF ROUGH SEA SURFACE

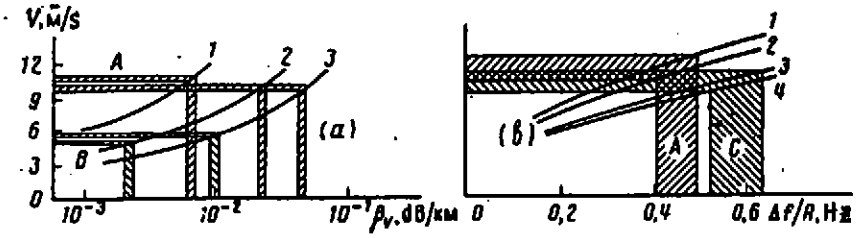

Fig.4 Determination of wind velocity V from β_V at three frequencies (1-3) on path II and at two frequencies (2,3) on path III (a) and from Δf_V /R at two frequencies on paths II and IV (b). A is path II, B is III, and C is path IV. The experimental values of β_V and Δf_V are given with the error obtained by sampling standart deviations of β, β_{sw}, Δf, Δf_o, and Δf_{sw} taken into account. The theoretical dependences of β_V and Δf_V /R are calculated for particular experimental conditions using the equations taken from [5,7] for the roughness spectrum with the Pierson-Moskovitz frequency dependence and an isotropic angular distribution of energy. 1 - 300 km, 2 - 400 km, 3 - 830 km, 4 - 950 km.

IV we defined the ratio Δf_V / R, where $R=(f_i/f_o)^{1.8}$, which, as follows from the experiment and theoretical calculation, is practically independent of frequency. From Δf_V /R we found the average wind velocity on the path V =9.5 - 12 m/s (see Fig. 4b).

The average swell parameters and wind velocities on the path, obtained by acoustic measurements agree well with the synoptic data. This confirms the initial theoretical premises [1,5-7,10] and shows that the estimates of the roughness parameters (except for $\Delta\psi$) are rather stable with respect to errors in measurement.

REFERENCES

[1] L M BREKHOVSKIKH & Yu P LYSANOV, 'Theoretical Fundamentals of Ocean Acoustics' Moscow, Gidrometeoizdat 1982. 262 p
[2] I B BURLAKOVA, YU A DUBOVOY, A L ZEIGMAN and et al, 'About Posibility of the Acoustic Tomography of the Rough Sea Surface',

ACOUSTIC TOMOGRAPHY OF ROUGH SEA SURFACE

Akustichesky Zhurnal, 34, No 3, 423-430 (1988)
[3] J H MILLER, J F LYNCH, CHING-SANG CHIU, 'Estimation of Sea Surface Spectra Using Acoustic Tomography', JASA, 86, No 1, 326-345, (1989)
[4] V V PIKALOV & N G PREOBRAZHENSKY, 'Reconstruction Tomography in Gas Dynamics and Plasma Physics' Novosibirsk, Nauka, 1987, p231
[5] D I ABROSIMOV, L S DOLIN & A G NECHAYEV, 'Mean Field Attenuation at Waveguide Sound Propagation in Rough Ocean', Akustichesky Zhurnal, 31, No 4, 511-512 (1985)
[6] F I KRYAZHEV & V M KUDRYASHOV, 'Scattering Influence at the Boundary on the Sound Field in a Waveguide', Problems of Ocean Acoustics, Ed. L M Brekhovskikh & I B Andreyeva Moscow, Nauka, 1984, p57-59
[7] A G NECHAYEV, 'Field and Intensity Fluctuations of Acoustic Signal in Rough Ocean, Preprint No 123, Inst.Appl.Phys., Acad.Sci.USSR Gorky, 1985. 29 p
[8] A N TIKHONOV & V Ya ARSENIN, 'Methods for Solution of Incorrect Problems', Moscow, Nauka, 1979, p287
[9] W J PIERSON & H A MOSKOVITZ, 'A Proposed Spectral Form for Fully Developed Wind Sea Based on the Similarity Theory of S A Kitaigorodsky, J Geophys Res 69, No 24, 5181-5190 (1984)
[10] I B ANDREYEVA, 'Sound Scattering by Ocean Surface and Surface Layer. Ocean Acoustics. A State-of-the-Art Analysis' Ed. L M Brekhovskikh & I B Andreyeva, Moscow, Nauka,1982, p118-132
[11]I B BURLAKOVA, A L ZEIGMAN, A G NECHAEV, M M SLAVINSKY, 'Sound Propagation in the Ocean with Rough Surface',Acoustica of the Ocean Media, Moscow, Nauka, 1989, p64-75
[12] A L VIROVLYANSKY, A I SAICHEV & M M SLAVINSKY, 'On Spectrum of the Signal Received by a Moving Receiver in an Underwater Sound Channel', Akustichesky Zhurnal, 31, No 1, 22-26 (1985)
[13] R A VADOV, ' Low-Frequency Sound Attenuation in the Ocean Problems of Ocean Acoustics'. Ed L M Brekhovskikh & I B Andreyeva Moscow, Nauka, 1984, p31-42

Proceedings of the Institute of Acoustics

DOPPLER TOMOGRAPHY OF THE OCEAN BOTTOM

M M Slavinsky, Yu V Petukhov, I B Burlakova

Institute of Applied Physics, 46 Uljanov Street, Nizhny Novgorod, USSR

The present paper demonstrates the potentials of Doppler tomography for determination of angular dependence of the reflection coefficient for the even bottom, which yields the sound speed and sediment density; the authors have made some use of the results obtained in [1,2].

Theoretical analysis is made for a path-uniform ocean waveguide with a certain dependence of the sound speed $c(z)$ on depth $0 < z \leq H$, and constant density within the water layer ρ; the ocean bottom is modelled by a uniform liquid half-space with corresponding acoustic characteristics c_g and ρ_g. If a tonal source with radiation frequency $f_0 = \omega_0/2\pi$ moves in a well-defined horizontal direction $r = vt$ $(t \geq 0)$ at the depth z_s with speed v $(v/c_0 \ll 1)$, dependence of pressure $P(t)$ perturbation on time $t(r)$ at a stationary receiver placed at the depth z_r is defined by the signals propagating along "water" rays and rays with various nultiplicities $m = 1,2,\ldots$ of bottom reflections; correspondingly, signal frequencies depend on r (see [1,2]). Since further we will consider bottom reflections only, then in the case of $z_s/H \ll 1$ and $z_r/H \ll 1$ being most convenient for their separation by frequency Doppler shifts, each reflection will be formed by fours of signals with the same multiplicity m. Hence, after "current" spectral analysis of the signal $s(\omega,r) = \frac{1}{T}\int_t^{t+T} (\tau)\exp(i\omega\tau)\,d\tau$ and averaging T with respect to time, we find the following equation for spectral density of the power current $|S^{(m)}(\omega,r)|^2$ within the geometric-acoustic approximation of field presentation as multiple scattering:

$$|S^{(m)}(\omega,r)|^2 = R_0^2 \left| S_{1m}(\omega) V^m(\theta_{1m}) \frac{e^{i\frac{\omega}{c_s}\varphi_{1m}}}{\Sigma_{1m}^{1/2}} - \right. \qquad (1)$$

$$\left. - S_{2m}(\omega)\, V^m(\theta_{2m})\, \frac{e^{i\frac{\omega}{c_s}\varphi_{2m}}}{\Sigma_{2m}^{1/2}} - S_{3m}(\omega)\, V^m(\theta_{3m})\, \frac{e^{i\frac{\omega}{c_s}\varphi_{3m}}}{\Sigma_{3m}^{1/2}} + \right.$$

$$+ S_{4m}(\omega)\, V^{m}(\theta_{4m}) \left| \frac{e^{i\frac{\omega}{c_s}\varphi_{4m}}}{\Sigma^{1/2}} \right|^2 ,$$

where

$$\Sigma_{jm} = \sqrt{n^2(z_s) - \sin^2\theta_{jm}^{(0)}}\ \sqrt{n^2(z) - \sin^2\theta_{jm}^{(0)}}\ \Big/ \left[\sin\theta_{jm}^{(0)} \Big/ r_{jm} \left| \frac{\partial r_{jm}}{\partial \sin\theta_{jm}^{(0)}} \right| \right] ,$$

$$r_{jm} = 2m\,D(H) - r_j, \qquad r_1 = D(z_s) + D(z_r),$$

$$r_2 = D(z_r) - D(z_s), \qquad r_3 = -r_2, \qquad r_4 = -r_1;$$

$$\varphi_{jm} = 2m\,J(H) + \sin\theta_{jm}^{(0)} r - x_j, \qquad x_1 = J(z_s) + J(z_r),$$

$$x_2 = J(z_r) - J(z_s), \qquad x_3 = -x_2, \qquad x_4 = -x_1;$$

$$D(z) = \int_0^z \frac{\sin\theta_{jm}^{(0)}\,dz}{\sqrt{n^2(z) - \sin^2\theta_{jm}^{(0)}}} ,$$

$$J(z) = \int_0^z \sqrt{n^2(z) - \sin^2\theta_{jm}^{(0)}}\,dz ,$$

$$S_{jm} = \frac{1}{2\sqrt{\pi}\,\Omega_{jm}} \exp\left\{ -\left(\frac{\omega - \omega_{jm}}{\Omega_{jm}} \right)^2 \right\} ,$$

$$\omega_{jm} = \omega_0 \left[1 - \frac{v}{c_s} \sin\theta_{jm}^{(0)} \right] ,$$

DOPPLER TOMOGRAPHY OF THE OCEAN BOTTOM

$$V(\theta_{jm}) = \frac{\mu_g \cos\theta_{jm} - \sqrt{n_g^2 - \sin^2\theta_{jm}}}{\mu_g \cos\theta_{jm} + \sqrt{n_g^2 - \sin^2\theta_{jm}}},$$

$$n_g = \frac{c(H)}{c_g}, \quad \mu_g = \frac{\rho_g}{\rho}.$$

Here $n(z) = c(z_s)/c(z)$ is refraction index for acoustic waves, $c_s = c(z_s)$, $\theta_{jm}^{(o)} < \arcsin[n(H)]$ is the emission angle of the corresponding ray, being the solution of the equation for the stationary phase point, $r_{jm}(\theta_{jm}^{(o)}) = r$, $\theta_{jm} = \arcsin[\sin\theta_{jm}^{(o)}/n(H)]$, the angle of incidence at the bottom; $S_{jm}(\omega)$, signal spectrum at the short distance R_o, Ω_{jm}, parameter characterizing spectrum width of the signal propagating along the corresponding ray, $V(\theta_{jm})$, Fresnel coefficient of wave reflection from the liquid bottom. Taking no account of small at $z_s/H \ll 1$ and $z_r/H \ll 1$ differences of angles of incidence $\theta_{jm} \approx \theta_m$ and amplitudes $\Sigma_{jm} \approx \Sigma_m$ of the four of rays $j = [1,4]$ forming the bottom reflection of multiplicity m, we find an easy-to-analyze expression from (1):

$$|S^{(m)}(\omega,r)|^2 = 4\frac{R_o^2}{\Sigma_m}|S_m(\omega)|^2\,|V(\theta_m)|^{2m}\cdot$$

$$\left\{1 - \cos\left[\frac{\omega}{c_s}2J(z_s)\right] - \cos\left[\frac{\omega}{c_s}2J(z)\right] + \right. \qquad (2)$$

$$\left. + \frac{1}{2}\cos\left[\frac{2\omega}{c_s}\left(J(z) - J(z_s)\right)\right] + \frac{1}{2}\cos\left[\frac{2\omega}{c_s}\left(J(z) + J(z_s)\right)\right]\right\}$$

which is further simplified at $z_s = z_r = z$:

$$|S^{(m)}(\omega,r)|^2 = 16\frac{R_o^2}{\Sigma_m}|S_m(\omega)|^2\,|V(\theta_m)|^{2m}\sin^4\left[\frac{\omega}{c(z_s)}2J(z)\right], \qquad (3)$$

Here

$$\Sigma_m = \sqrt{n^2(z_s) - \sin^2\theta_m^{(o)}}\,\sqrt{n^2(z) - \sin^2\theta_m^{(o)}}\;\Big/$$

$$\left[\sin\theta_m^{(o)}\Big/ r_m \;\left|\frac{\partial r_m}{\partial \sin\theta_m^{(o)}}\right|\right].$$

DOPPLER TOMOGRAPHY OF THE OCEAN BOTTOM

$$r_m = 2m\,D(H), \qquad \omega_{jm} \approx \omega_m = \omega_o\left(1 - \frac{v}{c_e}\sin\theta_m^{(o)}\right),$$

and emission angle $\theta_m^{(o)}$ is the solution of the equation $r_m = r$.

As follows from Eq. (2),(3), spectral density of power flow of bottom reflection signal with multiplicity m, i.e., $J_m(\omega,r) = \left(\frac{\Sigma_m}{R_o^2}\right)|S^{(m)}(\omega,r)|^2$, normalized to geometric divergence is a function oscillating with a period which increases as the distance grows; maxima of the function correspond to the spatial (angular) dependence of the reflection coefficient modulus to the power equal to doubled reflection multiplicity. Comparing Eqs. (2) and (3), it is obvious that the latter is more convenient to determine the angular dependence $|V(\theta_m)|^{2m}$, since all the interference maxima characterized by the last multiplier in Eq. (3) have the same amplitude, unlike in Eq. (2).

Thus, having obtained the experimental dependence $J_m(\omega_m,r)$ we can find its maxima and, consequently, develop a corresponding angular dependence $|V(\theta_m)|^{2m}$ whose accuracy for given H grows with increase of the emission frequency, depth of corresponding points, and bottom reflection multiplicity; that is, their increase causes the oscillation period $J_m(\omega_m,r)$ to decrease with respect to r, and angular dependence of the reflection coefficient is defined in more detail. Using $|V(\theta_m)|^{2m}$ to determine the angle of full internal reflection θ_r and $W_o = 1 - V(\theta_m = 0)$ we find the looked for parameters

$$n_g = \sin\theta_r, \qquad \mu_g = (2 - W_o)\,n/W_o$$

Of course, when obtaining experimental dependences $J_m(\omega_m,r)$ it is necessary to average $J_m(\omega_m,r) = (\Delta\omega)^{-1}\int_{\omega_m+\Delta\omega/2}^{\omega_m+\Delta\omega/2} J_m(\omega,r)\,d\omega$ with respect to a certain frequency band $\Delta\omega$ including Doppler frequency shifts for the four of signals with the correponding reflection multiplicity.

Now we will consider experiment testing of the proposed method for determining $V(\theta)$ and ground parameters c_g and ρ_g. Similar to [1-2], experimental investigations were made in a deep-water (H =

DOPPLER TOMOGRAPHY OF THE OCEAN BOTTOM

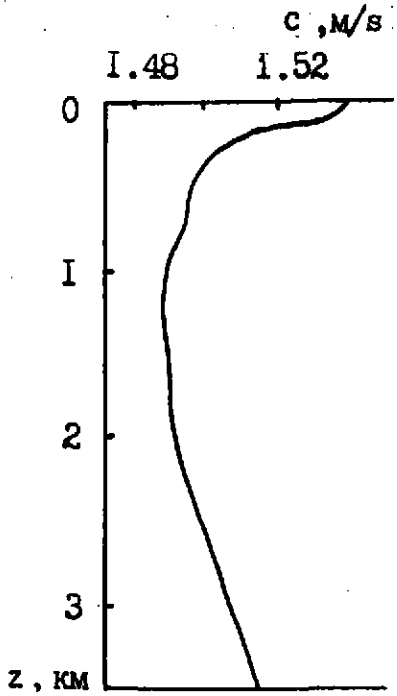

Fig. 1

$3.5 \cdot 10^3$ m) region of the Indian Ocean (Arabic Sea) with typical dependence of sound speed c(z) on depth (see Fig. 1) and even bottom whose upper sediment layer consists of silt and sand. The source emitted low- (f_o = 146 Hz) and high- (f_o = 392 Hz) frequency signals and was towed with velocity v = 3.5 - 4 m/s at depth z_s = 70 - 80 m. Acoustic signals were received at the depth z_r = 10^2 m. When experimental dependences on the distance of Doppler frequency shifts $\Delta f_m = \frac{\omega m}{2\pi} - f_o$ and corresponding to them - $J_m(\omega_m, r) = J_m(r)$ were determined for bottom reflections of various multiplicities m = 1,2,... the received signal p(t) was recorded in parallel to the reference one, heterodyned over intermediate frequency f_n = 1 Hz and filtered within the frequency band Δf_f = 2 Hz. The treated signal $p_f(t)$ was digitized and entered into the computer; digitization frequency was f_g = 5 Hz. Spectral analysis was made with no weight processing and with duration of each realization T = 10^2s and time step ΔT = 25 s ($t = l\Delta T$; l = 0,1,...)

Dependence $W(\Delta f, r) = \frac{1}{T}\int_t^{t+T} p_f(t)\, e^{i\Delta\omega t} dt$ shown in Fig. 2 only at high frequency f_o = 392 Hz for the sake of ease of interpretation yields the following: in the plane (Δf - r) (Doppler frequency shift - distance) trajectories $\Delta f_0(r)$, $\Delta f_1(r)$ and $\Delta f_2(r)$ are identified as well as bottom reflections with various multiplicities m = 1 and m =2. The trajectory $\Delta f_0(r)$ correspond to signals propagating along "purely" water rays.

Dependences $J_1(\omega_1, r)$ and $J_2(\omega_2, r)$ on r found after integration along corresponding trajectories $\Delta f_1(r)$ and $\Delta f_2(r)$ for both frequencies in two paths, are presented in Figs. 3, 4. Maxima of the dependences shown in those figures have been used to approximate the searched for angular dependences $J_m(r) = J_m(\omega_m, r)$ on r. We determined the following acoustic parameters of the bottom: $\rho_g/\rho_o \approx 1.66$, $c_o/c_g \approx 0.89$ at low frequency and $\rho_g/\rho_o \approx 1.6$, $c_o/c_g \approx$

0.95 at high frequency. They are in good agreement for m = 1 and m = 2 and seem to be sufficiently close to reality for both paths in this region of the ocean. The ratios ρ_g/ρ_o and c_g/c_o considerably decrease with increasing frequency; evidently, it is caused by the influence on reflection of higher-frequency sound of less deep layers of sediment thickness, on the average, with smaller c_g and ρ_g. Presented theoretical and experimental results are a proof for successful use of Doppler tomography combining aperture synthesis with Doppler effects, for determination of angular dependence of the bottom reflection coefficient, as well as of sound speed and density in sediments of deep-water ocean regions.

REFERENCES

[1] I B Burlakova, V N Golubev, A I Zharov, A G Nechaev, Yu V Petukhov, M M Slavinsky. Doppler tomography in ocean acoustics. Acoust. Zhourn., 34, N 4, p756-758 (1988)(in Russian).

[2] I B Burlakova, Yu V Petukhov, M M Slavinsky. Determination of acoustic characteristics of the ocean waveguide bottoms by the Doppler tomography method. Acoust. Zhourn.,35, N 6, p 1015-1020 (1989) (in Russian).

DOPPLER TOMOGRAPHY OF THE OCEAN BOTTOM

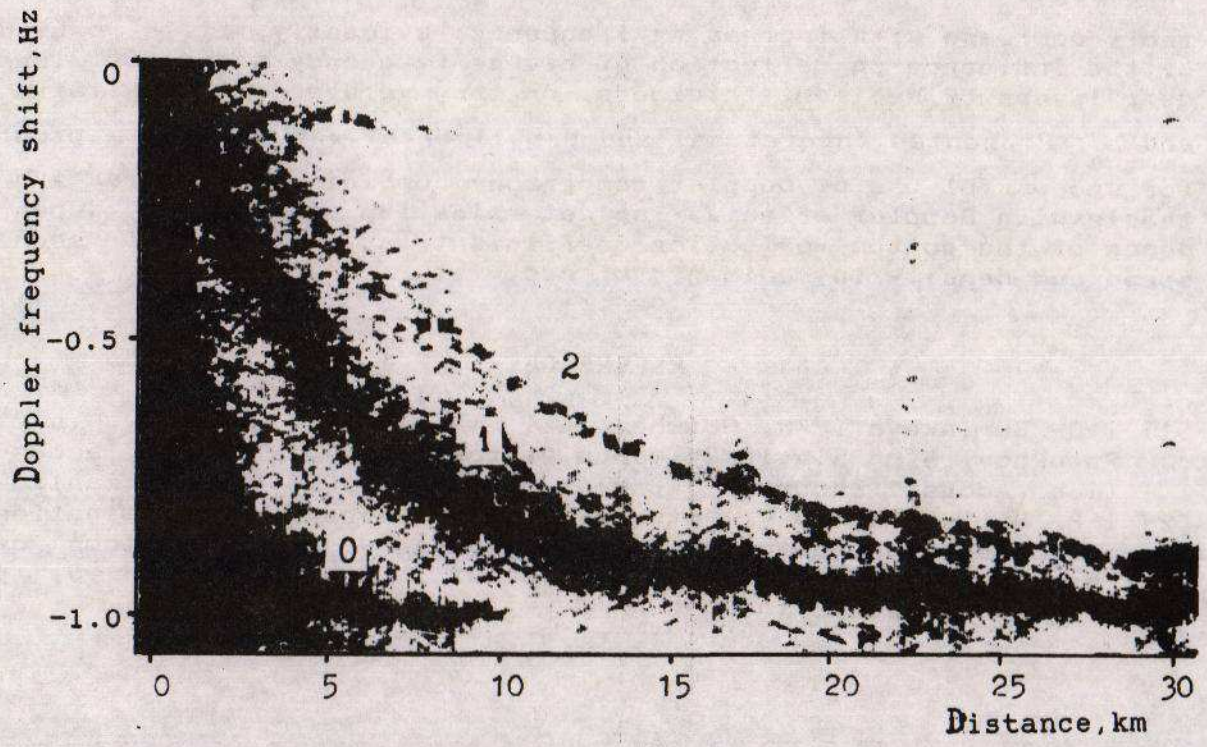

Fig. 2. Spectral density of acoustic signal power flow W(f,r) for radiation frequency f_0 = 392 Hz, presented as density record on the plane Doppler frequency shift - distance. Trajectories 0, 1, 2 correspond to Doppler frequency shifts $\Delta f_m(r)$ in water signals m = 0 and signals of the corresponding multiplicity m = 1, 2 of bottom reflections.

DOPPLER TOMOGRAPHY OF THE OCEAN BOTTOM

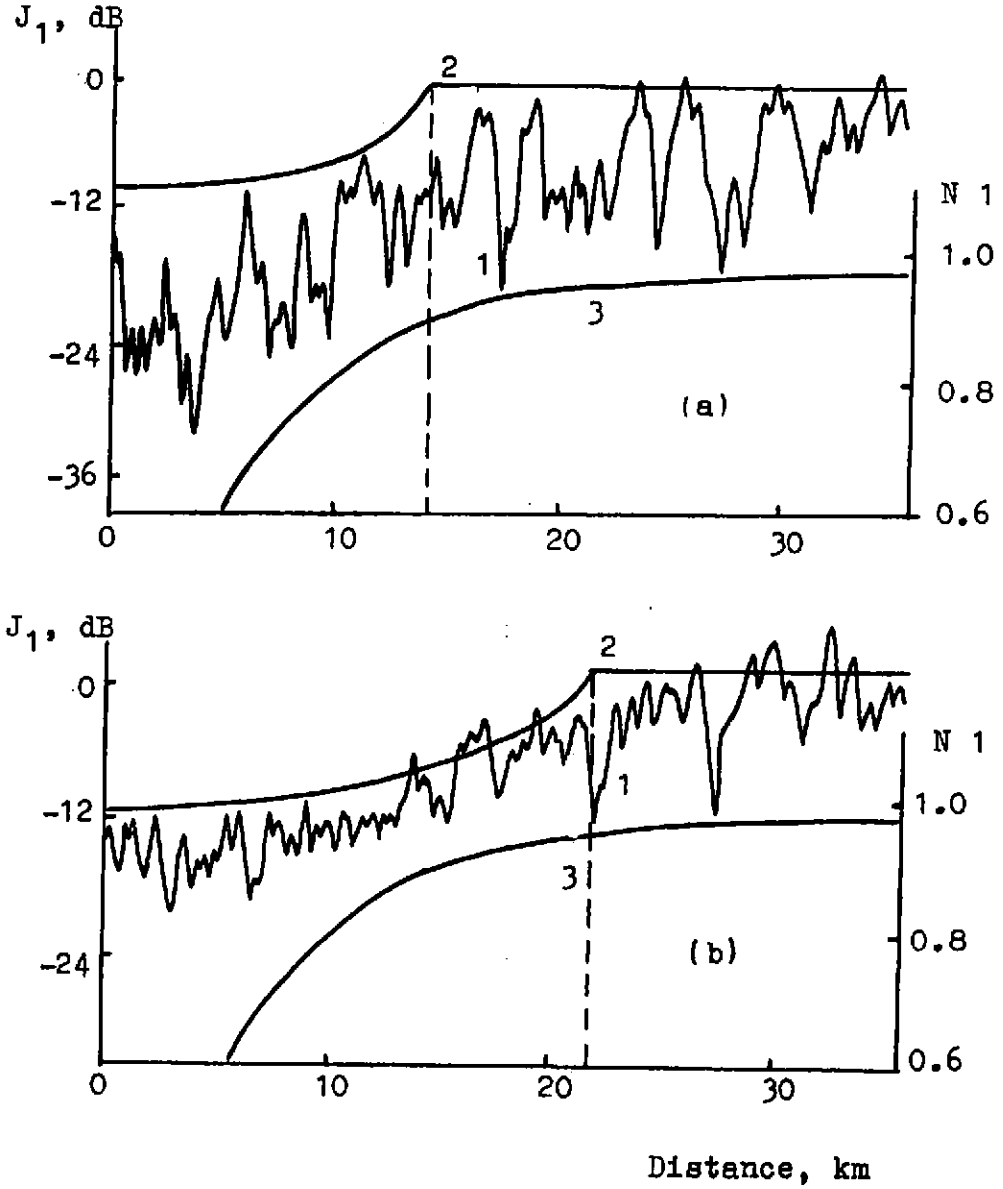

Fig. 3 f_0 = 146 Hz - (a); f_0 = 392 Hz - (b)

N 1 = $\sin\theta_1$

DOPPLER TOMOGRAPHY OF THE OCEAN BOTTOM

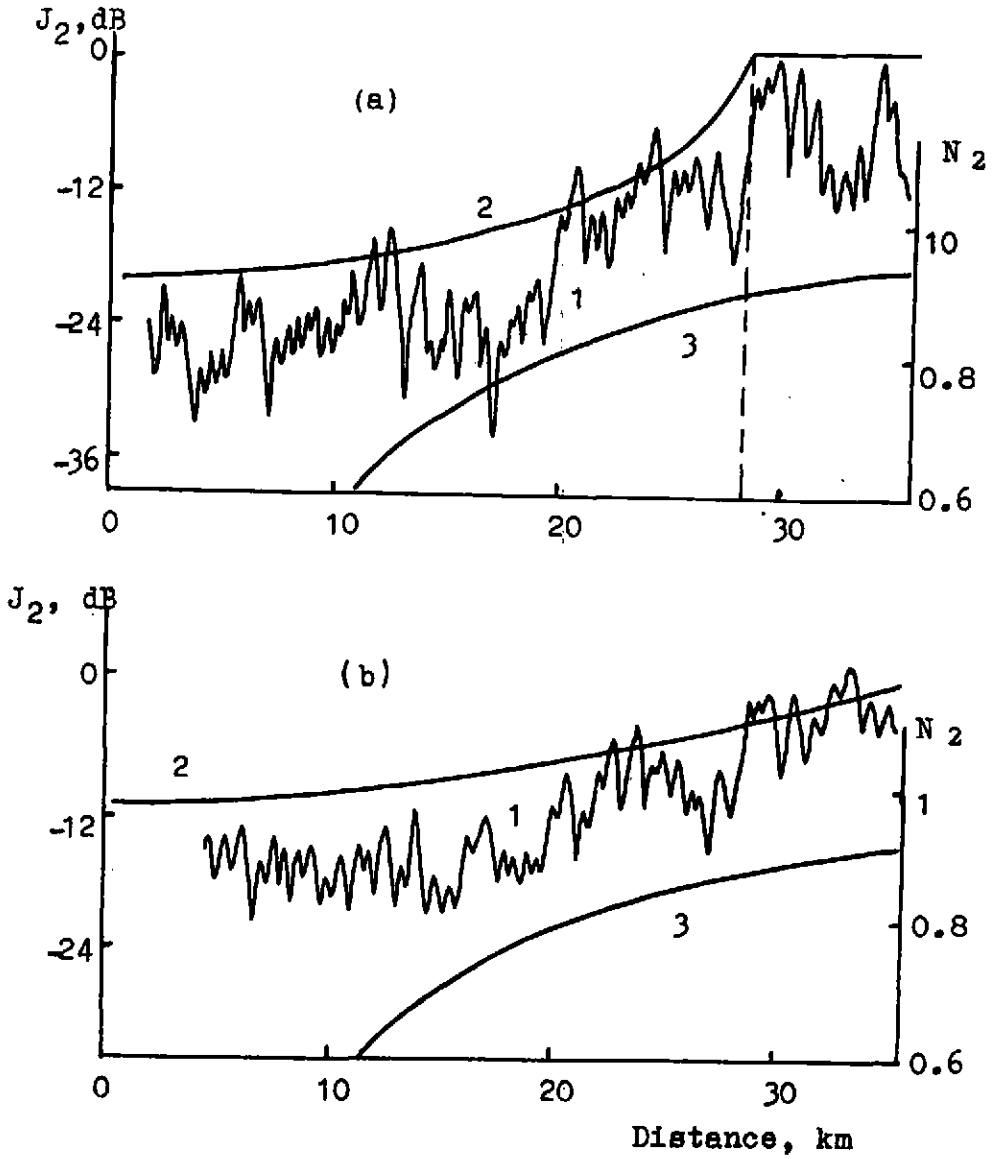

Fig. 4. f_0 = 146 Hz - (a); f_0 = 392 Hz - (b)

$N_2 = \sin \theta_2$